We are IntechOpen, the world's leading publisher of Open Access books Built by scientists, for scientists

6,900
Open access books available

186,000
International authors and editors

200M
Downloads

Our authors are among the

154
Countries delivered to

TOP 1%
most cited scientists

12.2%
Contributors from top 500 universities

CLARIVATE ANALYTICS
BOOK CITATION INDEX
INDEXED

WEB OF SCIENCE™

Selection of our books indexed in the Book Citation Index
in Web of Science™ Core Collection (BKCI)

Interested in publishing with us?
Contact book.department@intechopen.com

Numbers displayed above are based on latest data collected.
For more information visit www.intechopen.com

Enhanced Control of Carbon Nanotube Properties Using MPCVD with DC Electrical Bias

Placidus Amama[1,2*], Matthew Maschmann[1,3*] and Timothy Fisher[1,4]
[1]Air Force Research Laboratory, Materials and Manufacturing Directorate, AFRL/RXB
[2]University of Dayton Research Institute
[3]Universal Technology Corporation
[4]Purdue University
USA

1. Introduction

The engineering properties of carbon nanotubes (CNTs) allow for an extraordinarily large potential application space including thermal management, integrated circuits, mechanical reinforcement, and medical devices, among others. CNTs are generally characterized by the quantity of concentric graphene shells comprising their cylindrical wall structure. CNTs consisting of a single graphene cylinder are characterized as single-walled CNTs (SWNTs), while multiple concentric graphene cylinders are called multi-walled CNTs (MWNTs). Typical diameters for SWNTs are approximately $1-3$ nm, while MWNTs diameters range from approximately 2 nm to greater than 100 nm. The unique atomic arrangement of a SWNT dictates that each atom resides on both the interior and exterior of the structure, with the atomic orientation defined by a chiral vector relating the fully traversed perimeter of the SWNT to the unit vectors of a graphene sheet. Two thirds of SWNT chiralities are electrically semi-conducting, exhibiting an electronic band gap inversely proportional to their diameter, while the remaining third are metallic. Though the transport properties of MWNTs are degraded relative to SWNTs by the wall-to-wall interactions, they may still exceed the properties of traditional macroscale materials such as copper or aluminum. Despite the advantageous properties offered by CNTs, their integration into functional materials and devices in a manner that maximizes their benefit remains a significant technical and engineering challenge. Specific applications may demand a unique blend of characteristics such as diameter, alignment, purity, density, and chirality to maintain proper operation. *In situ* morphology and orientation control of CNTs during synthesis represents a promising path towards selectivity of these device-specific requirements, especially for applications requiring CNTs with engineered properties to be synthesized directly on a fucntionalized substrate. We examine the role of dc electrical bias during mircrowave plasma-enhanced chemical vapor deposition (MPCVD) synthesis of SWNTs using alignment, spatial density, chirality, and purity as metrics of interest. Further, we demonstrate enhanced thermal and electrial transport properties of MWNTs realized with application of substrate bias during MPCVD synthesis.

---

[*] contributed equally to this work.

2. Plasma enhanced Chemical Vapor Deposition

There is a wide range of methods for producing CNTs such as laser ablation, arc discharge, pyrolysis, and chemical vapor deposition (Huczko, 2002; Rakov, 2000). Chemical vapor deposition (CVD) has emerged as the method of choice for producing CNTs because of its simplicity, flexibility and affordability as well as the potential for scalability and the precise control of CNT properties. In a typical CVD growth process, a carbon precursor such as a hydrocarbon gas is heated to 750-900°C in the presence of a suitable catalyst (e.g., Fe, Co, and Ni), and if all the other reaction conditions such as catalyst particle size, nature of the catalyst support, and gas composition are optimized, nucleation and growth of CNTs proceeds. The CVD process is highly unique because CNTs grow from catalyst 'seeds,' and several studies have shown that there is an intimate relationship between the catalyst properties and the nanotube properties (Amama, et al., 2005a; Hofmann, et al., 2003). In other words, with proper control of the catalyst properties, it is possible to grow CNTs of controlled properties via CVD (Amama, et al., 2007; Amama, et al., 2010; Crouse, et al., 2008; Maschmann, et al., 2005; Zhu, et al., 2010). As such, an appreciable amount of research is underway to fully understand catalyst evolution during synthesis (Amama, et al., 2010; Amama, et al., 2009; Kim, et al., 2010). The CVD process typically involves either thermally driven gas phase decomposition of a hydrocarbon gas (thermal CVD) or both thermal and plasma decomposition (plasma-enhanced CVD).

MPCVD growth has received significant attention mainly because of the potential for low temperature CNT synthesis required for compatiblity with standard nanofabrication and CMOS processes and the ability to produce highly graphitized, vertically aligned CNTs (Amama, et al., 2006a; Meyyappan, et al., 2003). A distinguishing feature of the MPCVD process is the presence of a highly reactive plasma environment, which enhances the decomposition of the hydrocarbon feedstock during CNT growth. The generation of highly energetic ions by the plasma and their subsequent transport to the growth surface are two critical factors that influence the growth properties (Yen, et al., 2005). Using the wide parameter space of the MPCVD, a key advantage over other CVD processes, low temperature growth (Amama, et al., 2006a; Boskovic, et al., 2002), CNT alignment (Maschmann, et al., 2006d), chiral (Li, et al., 2004) and diameter control (Amama, et al., 2006b) have been demonstrated. In many plasma-enhanced CVD studies, the plasma source used is microwave energy which is characterized by high plasma density with a resonant field that is able to concentrate the plasma, ensuring that significant electron loss to the surrounding does not occur (Yen, et al., 2005). The plasma intensity is controlled by the microwave power while the ion flux directed at the substrate may be controlled by a dc bias voltage applied to the growth substrate. These parameters operate indepdently in MPCVD and are capable of substantially altering the properties of CNTs.

3. Effect of DC electrical bias during SWNT synthesis

3.1 Negative polarity electrical bias

Strict vertical alignment of CNTs may be of significant advantage for many applications, including electron emitters, mechanical enhancement, and high-density electronics. Although direct synthesis of vertically aligned or vertically oriented SWNT arrays has been commonly reported in the literature (Iwasaki, et al., 2005; Maruyama, et al., 2005; Murakami, et al., 2004; Zhong, et al., 2005), most refer to a general packing of SWNTs of subsequent

density that the growth front advances and remains in plane with the originating growth substrate. Closer examination of these arrays clearly reveals that individual CNTs within the array exhibit significant waviness and inconsistent orientation with respect to the substrate. Gravity assisted thermal CVD synthesis has reportedly resulted in freestanding vertical SWNTs by orienting the growth substrate upside down such that the SWNT growth direction corresponds to the direction of the gravitation field during synthesis (Yeh, et al., 2006). The vertical orientation using the gravity assisted technique seems to diminish for growth times greater than 1.5 minutes, as the free tips of sufficiently long SWNTs contact and are retained by growth substrate due to thermal vibrations (Yeh, et al., 2007). Others have designed catalyst systems embedded within a modified porous anodic alumina (PAA) template. SWNTs originating from within isolated vertical pore will follow the pore axis toward its opening, resulting in a vertical orientation (Maschmann, et al., 2006a; Maschmann, et al., 2006b). Though this technique successfully aligns individual SWNTs within the confined vertical pores, the free ends of SWNTs emerging from the pores adhere strongly to the top horizontal PAA surface rather than maintaining vertical alignment. SWNT functionalization within the vertical pore structure has been achieved (Franklin, et al., 2009a; Franklin, et al., 2009b), though the misaligned SWNTs on the top surface of the template may be unattractive for some applications. Assembly of freestanding vertical SWNTs from solution post-synthesis is also achievable through electrophoresis into predefined vertical vias etched in a silicon nitride mask (Goyal, et al., 2008). This technique yields variable SWNT deposition with respect to overall occupancy of pores and the number of SWNTs deposited per occupied pore, and SWNTs requires magnesium nitrate hexahydrate to encourage improved substrate adhesion. Though these techniques successfully generate vertically aligned SWNTs, each requires either substrate manipulation or significant catalyst processing, which may be undesirable or impractical for practical application.

Chiral selectivity, with respect to metallic or semiconducting behaviour, is important for optimal operation of many types of devices. Metallic CNTs are obviously well suited for applications requiring high current carrying capacity, such as electrical interconnects (Close, et al., 2008; Kreupl, et al., 2002); however, they may also be advantageous in devices requiring high sensitivity to small electrical potential changes, such as electro-chemical biological sensors (Claussen, et al., 2009). Field effect transistors utilizing semiconducting SWNT channels have been extensively studied and have been found to exhibit ballistic electronic transport even at room temperature operation (Franklin and Chen, 2010). Application of SWNT transistors in electronics offer obvious dimensional and efficiency advantages, and significant research continues in this area with respect to device processing and characterization. The strong preferential growth of semiconducting (Li, et al., 2004) or metallic (Harutyunyan, et al., 2009) SWNTs to population densities greater than 90% chirality selectivity have been reported in the literature by utilizing remote RF plasma and control of gas composition during annealing, respectively. We demonstrate the preferential selectivity of both vertical alignment and semiconducting chirality through the use of negative polarity substrate bias applied during SWNT synthesis using MPCVD.

To investigate the influence of DC electrical bias on SWNT synthesis, a SEKI AX5200S MPCVD reactor with electrically grounded chamber walls, shown schematically in Fig. 1. A hollow stainless steel rod contacts the bottom surface of an otherwise electrically isolated graphite heater stage and delivers a dc potential via a voltage-controlled current source (Sorensen DCS600-1.7E). A K-type thermocouple embedded in the rod monitored the stage

temperature, while the growth substrate surface temperature was measured using a dual wavelength pyrometer (Williamson model 90). The silicon growth substrate rested on a 5.08-cm diameter, 3.30-mm thick molybdenum puck used to concentrate the plasma directly above the sample.
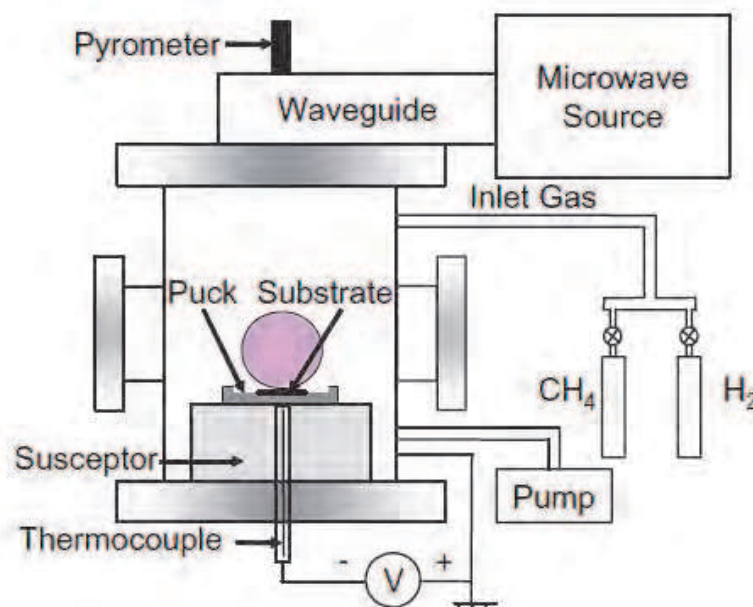

Fig. 1. Schematic of microwave plasma-enhanced chemical vapor deposition chamber.

An MgO supported Co catalyst was utilized for each SWNT synthesis. The catalyst particles were prepared by a wet mechanical mixing and combustion synthesis procedure using a solution of molybdenum, cobalt nitrate hexahydrate, and magnesium nitrate to produce bimetallic Mo/Co catalyst particles embedded in a nanoporous MgO support (Maschmann, et al., 2006d; Maschmann, et al., 2006c). The susceptor was first heated to 900°C in 50 sccm of flowing hydrogen at a pressure of 10 Torr. A dc substrate bias between 0 and -250 V was applied gradually to the substrate at a rate of approximately - 25 V/second after ignition of a 200 W microwave plasma. Methane was then introduced at a flow rate of 5 sccm to initiate CNT growth. Each synthesis was 20 minutes in duration. The surface temperature of the substrate recorded by the pyrometer was approximately 770°C and relatively insensitive to the applied bias.

Characterization of the SWNT product was performed using a Hitachi S-4800 field emission scanning electron microscope (SEM) and Senterra micro-Raman spectrometer. Laser excitation wavelengths of 533 and 785 nm were selected for recording Raman spectra, with at least ten locations examined for each sample. SEM characterization was utilized to assess SWNT relative alignment with respect to the growth substrate, SWNT length, density, and diameter estimates of individual SWNTs and SWNT bundles. Multi-excitation wavelength Raman spectra analysis allowed for quantification of SWNT quality, diameter distributions, and relative trends with respect to SWNT chirality.

The application of negative bias strengthens the electric field inherently present in the plasma sheath region immediately above the substrate, thereby accelerating the impingement of positively charged ions, such as H^+, towards the substrate. A plasma sheath is established as a result of the large mobility mismatch between ions and free electrons

generated within the plasma. The relatively low mass of electrons allows them to acquire a translational speed many times greater than that of the relatively heavy ions and accelerate away from the central concentrated plasma sphere located above the substrate.
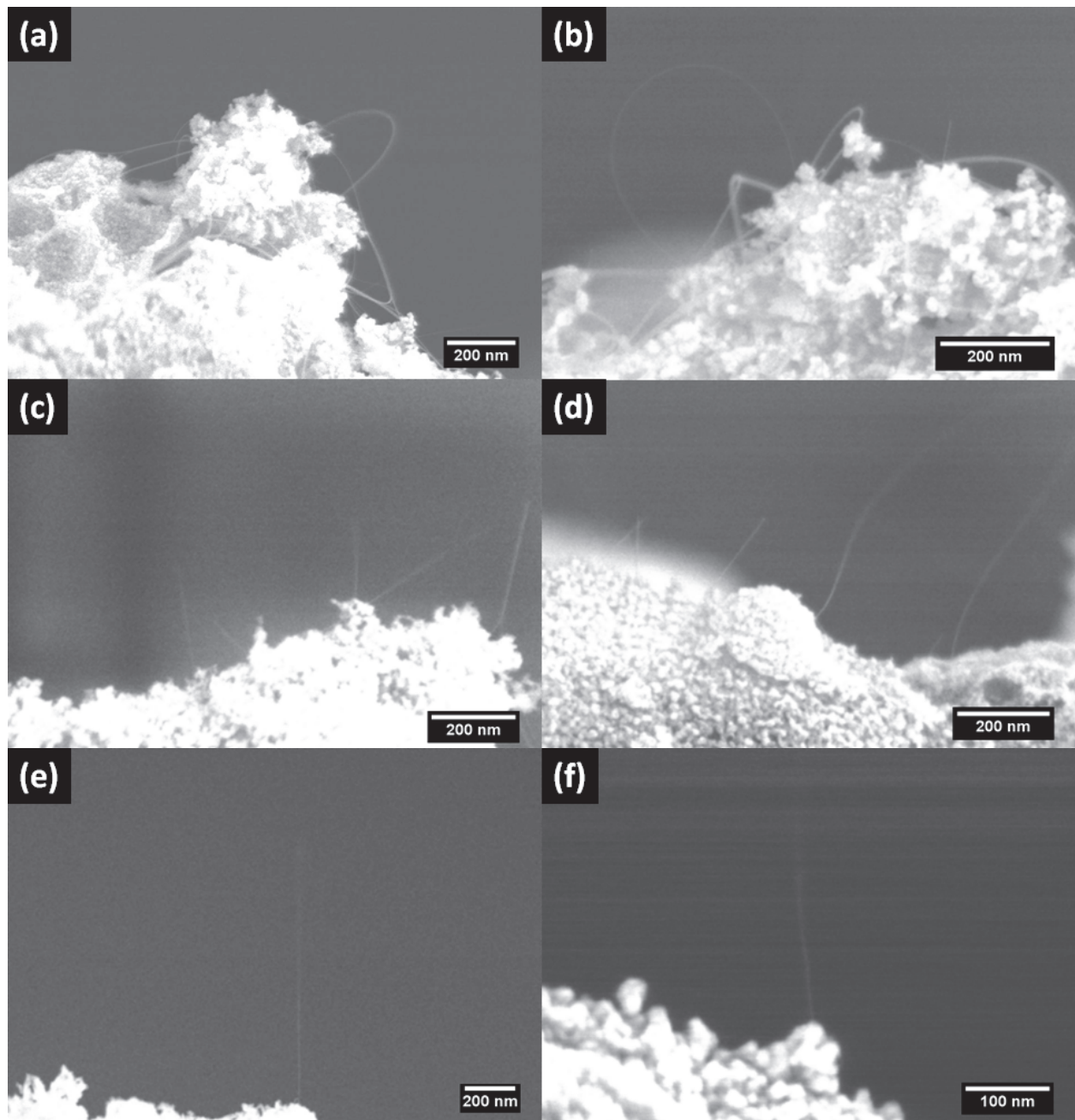

Fig. 2. Cross sectional SEM micrographs of SWNTs synthesized under negative polarity substrate bias in MPCVD at (a) 0V, (b) -50V, (c) -100V, (d) -150V, (e) -200V, and (f) -250V. From (Maschmann, et al., 2006d)

The bulk plasma is therefore electron deficient, setting up a net positive charge with respect to chamber walls, and an electric field is generated between the plasma and the surrounding surfaces. The highly anisotropic polarization of CNTs (Benedict, et al., 1995) establishes an interaction force between the CNT and the enhanced electric field near the growth substrate.

The magnitude of interaction is of sufficient magnitude to orient SWNTs (Peng, et al., 2003; Ural, et al., 2002; Zhang, et al., 2001) and multi-walled CNTs (Jang, et al., 2003; Merkulov, et al., 2001; Meyyappan, et al., 2003) along electric field lines *in situ* during CVD synthesis as well as during post-synthesis processing procedures (Kamat, et al., 2004; Yamamoto, et al., 1998).

Negative polarity substrate bias was systematically varied between 0 and -250V in 50V increments (Maschmann, et al., 2006d). Cross-sectional SEM analysis revealed distinct trends with respect to both SWNT spatial density and orientation relative to the growth substrate, as seen in Fig. 2a-f. SWNTs grown in the absence of applied bias or at -50V had a tendency to form large diameter bundles that generally followed the profile of the MgO support particles. No preferential growth perpendicular to the growth substrate was observed. The SWNTs synthesized at -100V and -150V, however, demonstrated a strong tendency to break free of the support particle in favor of a vertical orientation, normal to that of the support particles. SWNTs grown at these bias levels also tended to form bundles, with many longer SWNT bundles formed vertically oriented loops. A decrease in overall spatial density relative to the synthesis preformed without bias may also be discerned. At the greater bias magnitudes of -200V and -250V, a strong preference to vertical alignment is observed, in addition to a marked decrease in SWNT spatial density. Very few SWNTs were observed along the perimeter of the catalyst support particles, as is typically observed when bias is omitted from synthesis. Freestanding SWNTs with lengths of several microns were frequently observed, though the free tips of these SWNTs were often obscured by thermal vibrations.
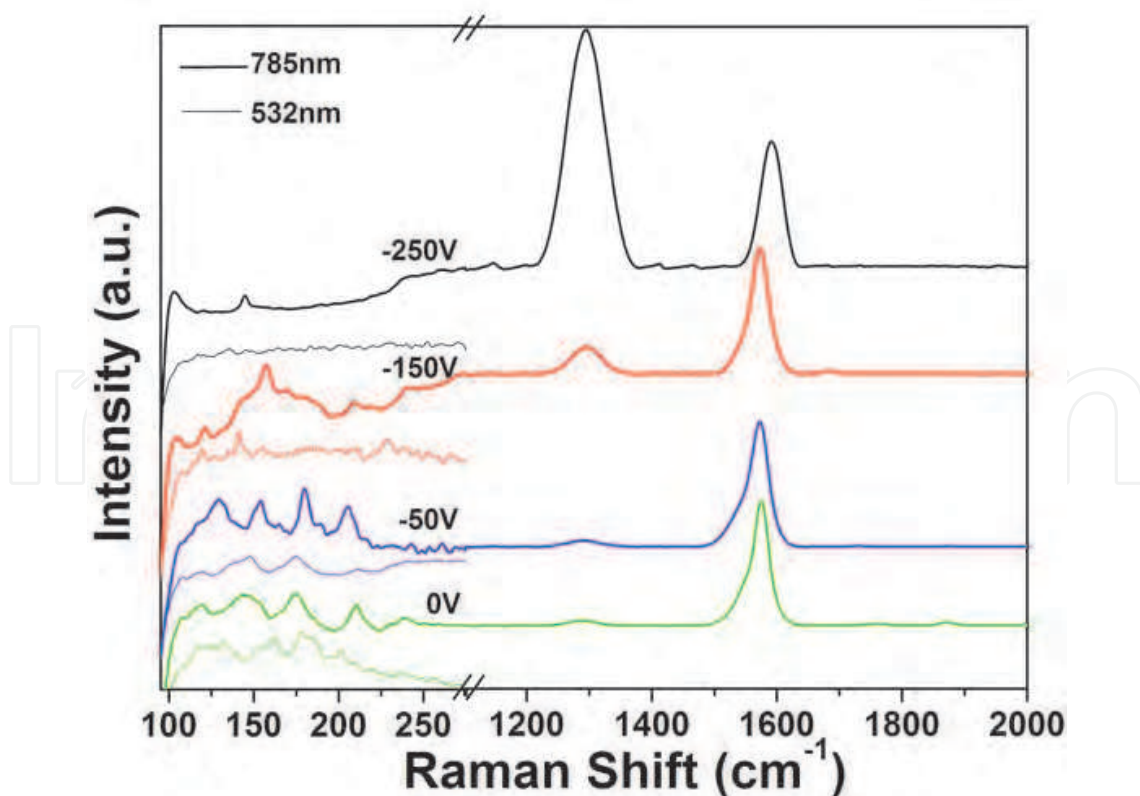

Fig. 3. Raman spectra of SWNTs synthesized using negative substrate bias in MPCVD. From (Maschmann, et al., 2006d).

Raman spectra of the SWNTs synthesized with negative polarity bias revealed another trend not readily observable from SEM observation, likely due to SWNT bundling and the inherent resolution limitations of the SEM. The radial breathing mode (RBM) distributions gradually skewed to lower frequency Raman shifts with increased levels of negative bias. Because SWNT diameter is inversely proportional to RBM frequency (Bachilo, et al., 2002; Rao, et al., 1997), the RBM distributions shift suggests a trend towards larger diameter SWNTs (up to 2.5 nm) as negative bias is increased. Locating the RBM peaks relative to excitation wavelengths on a Kataura plot (not shown) indicates that SWNTs synthesized without bias are a mix of metallic and semiconducting chiralities (Maschmann, et al., 2006d). Magnitudes of negative bias at and above -150V shift the measured RBM frequencies into bands of exclusively semiconducting chiralities. Additionally, a decreasing trend in the G- to D-band ratio is a further indication of a decreased spatial density observed by SEM and is perhaps an indication of an increased occurrence of SWNT wall defects. The Lorentzian lineshape of the G-band obtained from SWNTs under high levels of negative bias further support the RBM trend indicating a high concentration of semi-conducting SWNTs (Brown, et al., 2001; Pimenta, et al., 1998). The predominance of larger diameter SWNTs and corresponding decrease in SWNT density is thought to be a result of enhanced H^+ ion bombardment, which is known to preferentially etch small diameter SWNTs (Zhang, et al., 2005). Metallic SWNTs may have also been burned up as a result of transmitting a high current density.

3.2 Positive polarity electrical bias

Application of dc bias that is positive with respect to chamber walls is believed to decrease the magnitude of the electric field within the plasma sheath region near the growth substrate. H^+ ions, generated in abundance within the plasma, therefore attain a lower translational velocity before encountering the growth substrate. In fact, because the substrate in this configuration is the surface of greatest potential relative to the grounded chamber, the ions are instead more readily attracted toward the chamber walls. The mitigation of potentially harmful H^+ ion bombardment on the growth substrate is examined by varying the magnitude of positive polarity dc electrical bias during MPCVD SWNT synthesis, similarly to the methodology described in the previous section.

Substrate bias was varied between 0 and +200V in 50V increments while maintaining otherwise standard synthesis conditions. Bias levels of +250V or greater were attempted, but consistently led to plasma instabilities and were not further examined. Within the bias range of 0 and +100V, only incremental increases in SWNT spatial density were observed. SEM micrographs obtained from samples synthesized within this range of biases, shown in Fig. 4 (a) and (b), reveal SWNT bundles spanning tens of microns in length and tens of nanometers in diameter. No preferential vertical alignment of SWNTs is observed for these samples using cross-sectional SEM imaging (not shown). Larger biases of +150V and +200V resulted in dramatic increases in SWNT density, with a significant population of large-diameter SWNT ropes observed uniformly coating the support particle surfaces. Figures 4 (c-e) show typical SEM micrographs of SWNT products synthesized at +150 and +200V. The diameters of SWNT ropes often exceed 50 nm, with smaller feeder bundles ranging between 10-25 nm. Cross-sectional SEM analysis of these samples (Figure 4e) reveals that a small fraction of isolated SWNTs are freestanding and oriented in the direction normal to the support particle. Within the resolution limitations of the SEM, the vertical SWNTs synthesized at

+200V bias appear to be smaller in diameter than the vertical SWNTs synthesized using negative bias (Fig. 3c-f). The hypothesized weakened ion bombardment, even relative to the neutral 0V bias case, may encourage the synthesis of CNTs of all orientations that may otherwise be etched by H^+ ions, allowing these SWNTs to escape the bundling effect encountered by SWNTs that follow the profile of the support particles.
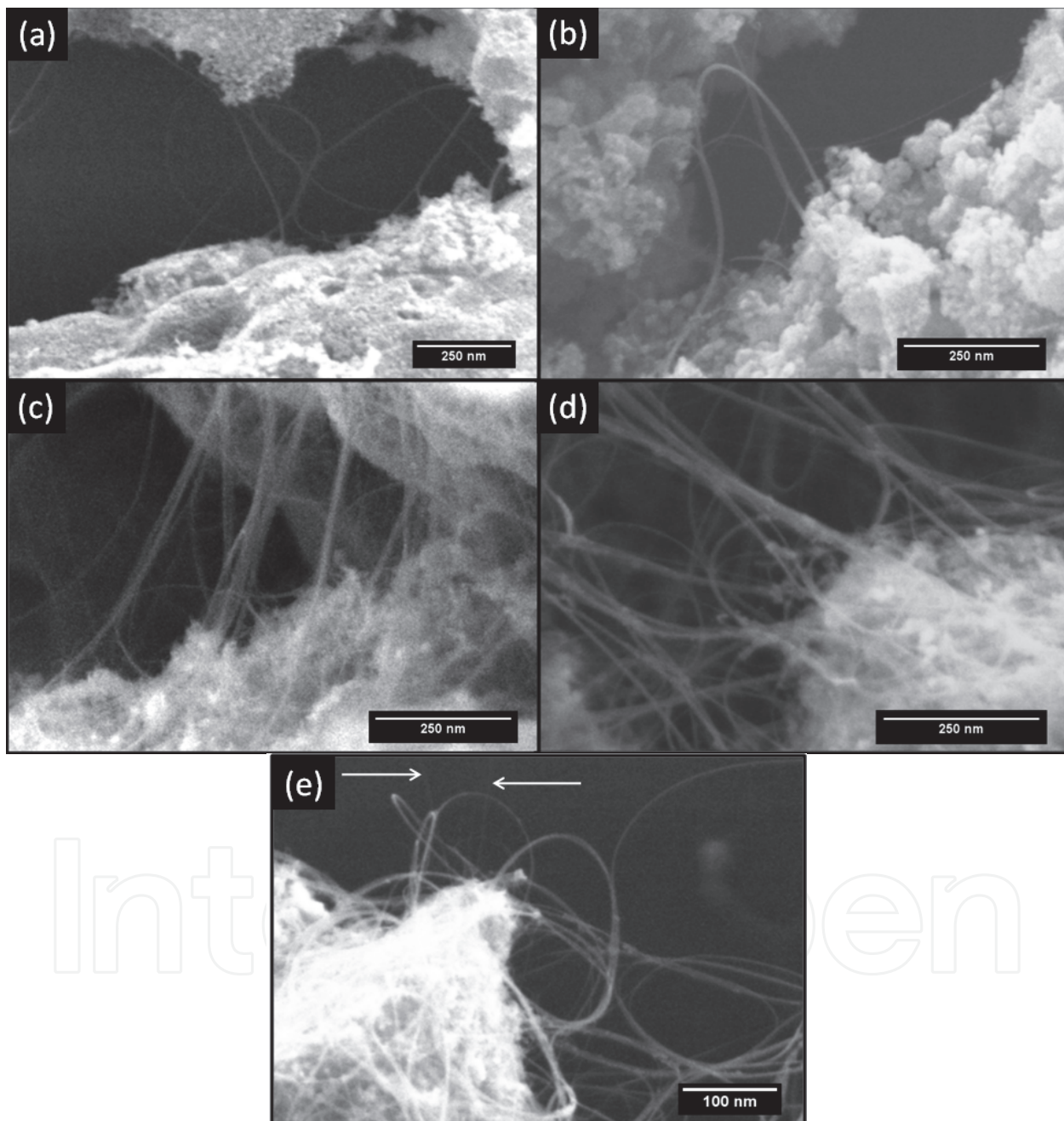

Fig. 4. SEM micrographs of SWNTs synthesized at (a) 0V, (b) +50, (c) +150, and (d-e) +200V substrate bias in MPCVD. Arrows indicate the presence of freestanding vertical SWNTs.

Raman spectroscopy yields further insights into the SWNTs produced using positive bias. While negative bias resulted in a shift in RBM peaks towards lower frequencies, the application of positive bias resulted in a shift in RBM peaks towards higher frequencies, as

shown in Fig. 5. RBMs in the range of $100 - 200$ cm^{-1} are present for all levels of positive bias for both 785 and 532 nm excitation wavelengths, but RBM frequencies greater than 250 cm^{-1} emerge at bias levels above +150V. Employing a 785 nm excitation wavelength, a RBM peak at 259 cm^{-1} emerges at +150V, while a peak at 261 cm^{-1} is present at +200V. Using a 532 nm excitation wavelength, a RBM peak at 251 cm^{-1} emerges at +200V. In terms of SWNT diameter distribution, the presence of these RBMs indicates the emergence of SWNTs with diameters less than 1 nm (Bachilo, et al., 2002; Rao, et al., 1997). As mentioned previously, this effect may be attributed to decreased H$^+$ ion bombardment which tends to preferentially etch smaller diameter SWNTs. A mixture of metallic and semiconducting chiralities exist, based on the location of RBM peaks on a Kataura plot (not shown), indicating that no chiral selectivity is attained using positive polarity bias.
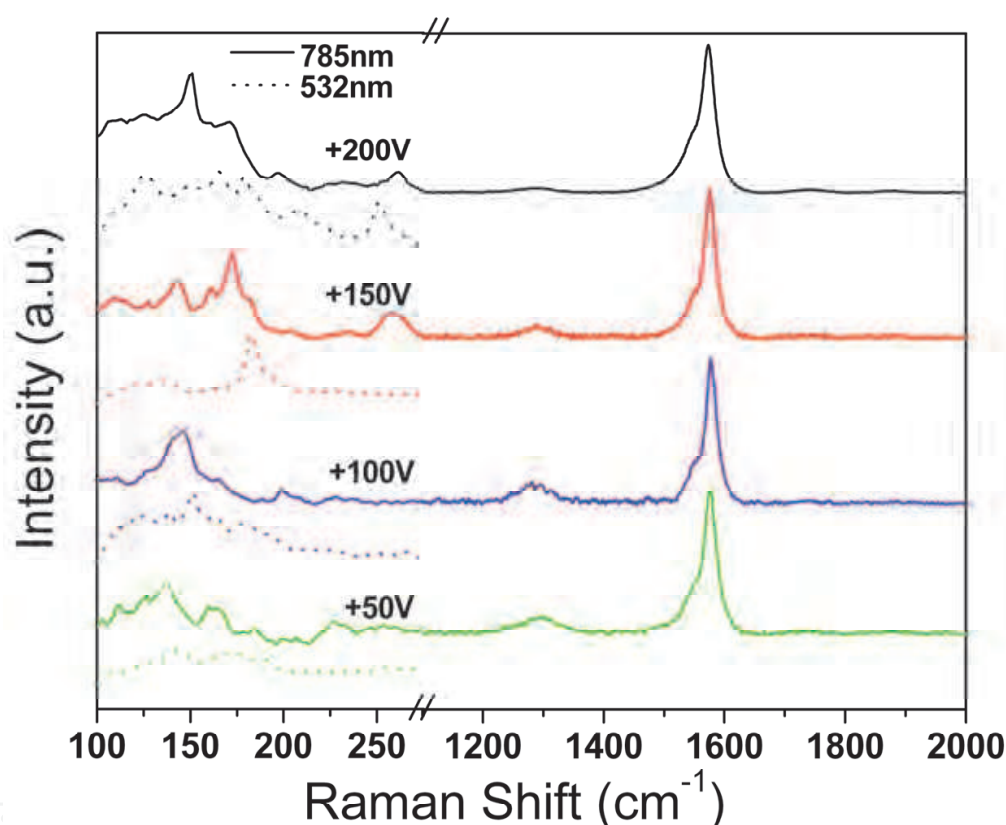

Fig. 5. Raman spectra for SWNTs synthesized using positive polarity bias in MPCVD.

Examination of the G-band further indicates a significant difference in composition of SWNTs grown under negative and positive bias. A Breit-Wanger-Fano line shape, appearing as a shoulder on the G-band at approximately 1550 cm^{-1} in Fig. 5, is indicative of metallic SWNTs (Brown, et al., 2001; Pimenta, et al., 1998) and is absent in G-bands obtained for SWNTs grown using negative bias (Fig. 3). Additionally, the G- to D-band ratios are substantially greater when utilizing positive bias. While application of negative bias attracts and accelerates H$^+$ ions to the growth substrate, thus damaging SWNT walls, the application of positive bias appears to adequately decrease the incoming velocity of H$^+$ ions to the substrate and may protect SWNTs from excessive ion bombardment. Consequently, the ratio of G- to D-band ratio for SWNTs grown using positive applied bias increased from approximately 10 for samples grown without bias to approximately 40 for those grown at

+200 V. Such a high ratio indicates a large quantity of high-quality SWNTs with little amorphous carbon.

4. Influence of DC electrical bias during MWNT synthesis

The influence of dc bias voltage during MPCVD synthesis of MWNTs from dendrimer-templated Fe_2O_3 nanoparticles will be discussed with respect to the the resulting thermal and electrial transport properties of MWNT arrays. The DC bias values exmained range from -200 to +200V, in 100V increments using similar experimental techniques discussed in the previous sections. The electrical resistance of the MWNTs were measured by obtaining the slope of I-V characterization of randomly selected individual MWNTs across lithographically defined Au/Ti electrodes. Five individual MWNTs were studied for each level of dc bias. The thermal performance was assessed by utilizing the MWNT arrays as a thermal interface. Thermal resistance of the CNT interface material was determined using a photoacoustic technique (Cola, et al., 2007). The thermal resistance measurement was performed at a single interface pressure of 10 psi. Three MWNT array interfaces from each synthesis bias level were produced and characterized.
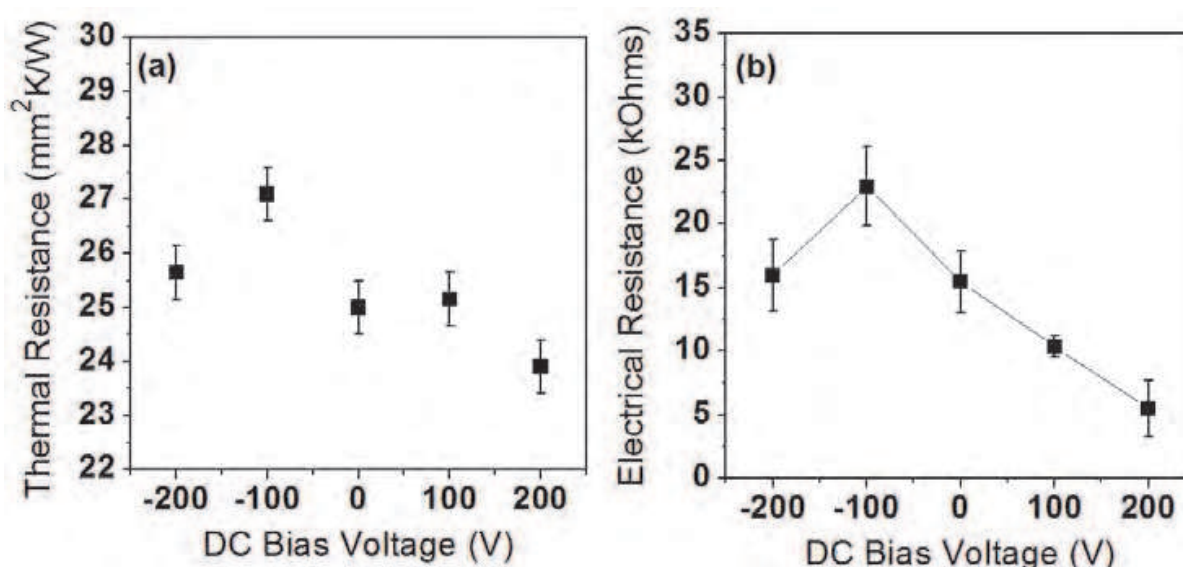

Fig. 6. Measured thermal interface resistance of MWNT arrays determined using a photoacoustic technique (a) and electrical resistance of individual MWNTs (b) as a function of dc bias voltage used during growth in the MPCVD. From (Amama, et al., 2008)

Figure 6 exhibits the electrical and thermal resistance values as a function of applied substrate bias during MPCVD synthesis. Similar trends with respect to substrate bias exist among the data sets, suggesting that similar phenomena during synthesis may be affecting both thermal and electrical transport. MWNTs grown under positive dc bias (+200V) demonstrate the lowest resistances, while the highest resistances were observed for MWNTs grown under negative dc bias voltage (-100V). The lowest thermal interface resistance (23.9 mm²/K/W) was observed for MWNT arrays grown under a dc bias voltage of +200 V while MWNT arrays grown at -100 V showed the highest thermal interface resistance (27.1 mm²/K/W). Similarly, the lowest electrial resistance (5.5 kOhms) was attained at +200V, while the greatest electrical resistance (23 kOhms). The electrical resistance data exhibits a

nearly linear decrease with respect to applied positive polarity bias, the thermal resistance observed at +100V was statistically equivalent to that observed at 0V bias. It is possible that the defect density present in MWNTs may contribute to the observed variation in electrical resistances as shown previously (Lan, et al., 2007).
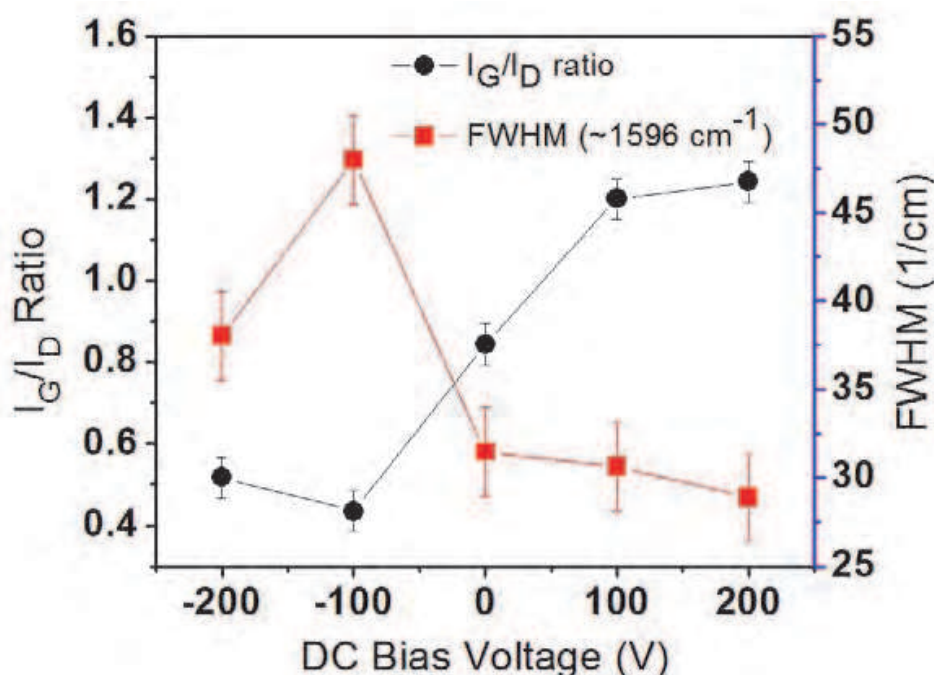

Fig. 7. Raman spectroscopy data obtained from MWNT arrays synthesized in MPCVD using dc substrate bias. I_G/I_D ratio represents the relative peak intensity ratio of the G-band to D-band, while the FWHM data is measured relative to the G-bank peak. From (Amama, et al., 2008).

The thermal and relectrical resistance trends are consistent with those exhibited by the G- to D-band ratio measured via Raman spectroscopy for the MWNT samples. As seen in Fig. 7, the relative ratio of the well graphitized carbon (G-band) to disordered carbon (D-band) steadily increases as a function of positive polarity dc bias. The ratio maxima occurs at +200V, consistent with the minimal thermal and electrical resistance measurments. The minima at -100V corresponds to the maximum observed thermal and electrical resistance. The observed behavior of the I_G/I_D ratio is consistent with the full width at half maximum (FWHM) of the G-band at ~1596 cm^{-1}. We hypothesize that negative dc bias voltage accelerated H$^+$ ions, introducing defects on the CNTs. This effect is most pronounced for MWNTs grown under -100 V. The relatively consistent trend between the measured resistance data and the Raman spectra data gives further evidence of this hypothesis. Biasing the substrate positively, on the other hand, reduces electric field near the substrate, reducing the bombardment of H$^+$ and other positively charged hydrocarbon ions generated in the plasma from the CNTs.

5. Conclusion

The parameter space for MPCVD synthesis of CNTs is vast, allowing a user a high level of fidelity with respect to control of CNT structure and morphology. The application of

substrate bias independently from plasma power and other growth parameters is a unique and robust feature of MPCVD that enables *in situ* control of CNT alignment, quality, density, and chirality and extends the potential application space for plasma-grown CNTs. We have demonstrated that both the polarity and magnitude of the applied bias dictate the resulting CNT yield. Negative polarity bias lends itself to vertical orientation and is a means to preferentially synthesize larger diameter semiconducting SWNTs. Conversely, positive polarity bias dramatically increases the SWNT quality and yield while resulting in a mix of metallic and semiconducting chiralities. To the detriment of the technique, however, the quality metrics seem exclusive to a given bias polarity. For example, the synthesis of high density, vertical freestanding SWNTs has, to date, been a challenge through variation of bias alone, and more research is required to fully optimize the capabilities of applied bias during SWNT synthesis. For MWNT synthesis, the alignment capability of negative polarity bias is well established, though the application of positive polarity bias remains relatively unexplored. We observe that positive polarity bias at levels greater than +100V during MPCVD synthesis appears to demonstrate a protective role, partially shielding CNTs from harmful ion bombardment. As a result, MWNTs exhibit enhanced thermal and electrical conductivity. The degree of freedom offered by substrate bias during MPCVD synthesis offers a tremendous extension to traditional CNT synthesis capabilities and potential inroads to myriad applications requiring strict control of SWNT or MWNT properties.

6. References

Amama, P. B.; Lim, S.; Ciuparu, D.; Yang, Y.; Pfefferle, L. & Haller, G. L. (2005a). Synthesis, Characterization, and Stability of Fe-MCM-41 for Production of Carbon Nanotubes by Acetylene Pyrolysis. *J. Phys. Chem. B*, 109, 7, pp. 2645-2656

Amama, P. B.; Ogebule, O.; Maschmann, M. R.; Sands, T. D. & Fisher, T. S. (2006a). Dendrimer-assisted low-temperature growth of carbon nanotubes by plasma-enhanced chemical vapor deposition. *Chem. Commun. (Cambridge, U. K.)*, 27, pp. 2899-2901

Amama, P. B.; Maschmann, M. R.; Fisher, T. S. & Sands, T. D. (2006b). Dendrimer-Templated Fe Nanoparticles for the Growth of Single-Wall Carbon Nanotubes by Plasma-Enhanced CVD. *J. Phys. Chem. B*, 110, 22, pp. 10636-10644

Amama, P. B.; Cola, B. A.; Sands, T. D.; Xu, X. F. & Fisher, T. S. (2007). Dendrimer-assisted controlled growth of carbon nanotubes for enhanced thermal interface conductance. *Nanotechnology*, 18, 38, pp. 385303-385306

Amama, P. B.; Lan, C.; Cola, B. A.; Xu, X.; Reifenberger, R. G. & Fisher, T. S. (2008). Electrical and Thermal Interface Conductance of Carbon Nanotubes Grown under Direct Current Bias Voltage. *J. Phys. Chem. C*, 112, 49, pp. 19727-19733

Amama, P. B.; Pint, C. L.; Mcjilton, L.; Kim, S. M.; Stach, E. A.; Murray, P. T.; Hauge, R. H. & Maruyama, B. (2009). Role of water in super growth of single-walled carbon nanotube carpets. *Nano Lett.*, 9, 1, pp. 44-49

Amama, P. B.; Pint, C. L.; Kim, S. M.; Mcjilton, L.; Eyink, K. G.; Stach, E. A.; Hauge, R. H. & Maruyama, B. (2010). Influence of Alumina Type on the Evolution and Activity of Alumina-Supported Fe Catalysts in Single-Walled Carbon Nanotube Carpet Growth. *ACS Nano*, 4, 2, pp. 895-904

Bachilo, S. M.; Strano, M. S.; Kittrell, C.; Hauge, R. H.; Smalley, R. E. & Weisman, R. B. (2002). Structure-Assigned Optical Spectra of Single-Walled Carbon Nanotubes. *Science*, 298, 5602, pp. 2361-2366

Benedict, L. X.; Louie, S. G. & Cohen, M. L. (1995). Static polarizabilities of single-wall carbon nanotubes. *Phys. Rev. B*, 52, 11, pp. 8541-8549

Boskovic, B. O.; Stolojan, V.; Khan, R. U. A.; Haq, S. & Silva, S. R. P. (2002). Large-area synthesis of carbon nanofibres at room temperature. *Nat. Mater.*, 1, 3, pp. 165-168

Brown, S. D. M.; Jorio, A.; Corio, P.; Dresselhaus, M. S.; Dresselhaus, G.; Saito, R. & Kneipp, K. (2001). Origin of the Breit-Wigner-Fano lineshape of the tangential G-band feature of metallic carbon nanotubes. *Phys. Rev. B*, 63, 15, pp. 155411-155418

Claussen, J. C.; Franklin, A. D.; Ul Haque, A.; Porterfield, D. M. & Fisher, T. S. (2009). Electrochemical Biosensor of Nanocube-Augmented Carbon Nanotube Networks. *ACS Nano*, 3, 1, pp. 37-44

Close, G. F.; Yasuda, S.; Paul, B.; Fujita, S. & Wong, H. S. P. (2008). A 1 GHz integrated circuit with carbon nanotube interconnects and silicon transistors. *Nano Lett.*, 8, 2, pp. 706-709

Cola, B. A.; Xu, J.; Cheng, C.; Xu, X.; Fisher, T. S. & Hu, H. (2007). Photoacoustic characterization of carbon nanotube array thermal interfaces. *J. Appl. Phys.*, 101, 5, pp. 054313-054319

Crouse, C. A.; Maruyama, B.; Colorado Jr, R.; Back, T. & Barron, A. R. (2008). Growth, New Growth, and Amplification of Carbon Nanotubes as a Function of Catalyst Composition. *J. Am. Chem. Soc.*, 130, 25, pp. 7946-7954

Franklin, A. D.; Sayer, R. A.; Sands, T. D.; Fisher, T. S. & Janes, D. B. (2009a). Toward surround gates on vertical single-walled carbon nanotube devices. *J. Vac. Sci. Technol., B*, 27, 2, pp. 821-826

Franklin, A. D.; Sayer, R. A.; Sands, T. D.; Janes, D. B. & Fisher, T. S. (2009b). Vertical Carbon Nanotube Devices With Nanoscale Lengths Controlled Without Lithography. *Nanotechnology, IEEE Transactions on*, 8, 4, pp. 469-476

Franklin, A. D. & Chen, Z. (2010). Length scaling of carbon nanotube transistors. *Nat Nano*, 5, 12, pp. 858-862

Goyal, A.; Liu, S.; Iqbal, Z.; Fetter, L. A. & Farrow, R. C. (2008). Directed self-assembly of individual vertically aligned carbon nanotubes. *J. Vac. Sci. Technol., B*, 26, pp. 2524-2528

Harutyunyan, A. R.; Chen, G.; Paronyan, T. M.; Pigos, E. M.; Kuznetsov, O. A.; Hewaparakrama, K.; Kim, S. M.; Zakharov, D.; Stach, E. A. & Sumanasekera, G. U. (2009). Preferential Growth of Single-Walled Carbon Nanotubes with Metallic Conductivity. *Science*, 326, 5949, pp. 116-120

Hofmann, S.; Ducati, C.; Robertson, J. & Kleinsorge, B. (2003). Low-temperature growth of carbon nanotubes by plasma-enhanced chemical vapor deposition. *Appl. Phys. Lett.*, 83, 1, pp. 135-137

Huczko, A. (2002). Synthesis of aligned carbon nanotubes. *Appl. Phys. A*, 74, 5, pp. 617-638

Iwasaki, T.; Zhong, G.; Aikawa, T.; Yoshida, T. & Kawarada, H. (2005). Direct Evidence for Root Growth of Vertically Aligned Single-Walled Carbon Nanotubes by Microwave Plasma Chemical Vapor Deposition. *J. Phys. Chem. B*, 109, 42, pp. 19556-19559

Jang, Y.-T.; Ahn, J.-H.; Ju, B.-K. & Lee, Y.-H. (2003). Lateral growth of aligned mutilwalled carbon nanotubes under electric field. *Solid State Commun.*, 126, 6, pp. 305-308

Kamat, P. V.; Thomas, K. G.; Barazzouk, S.; Girishkumar, G.; Vinodgopal, K. & Meisel, D. (2004). Self-Assembled Linear Bundles of Single Wall Carbon Nanotubes and Their Alignment and Deposition as a Film in a dc Field. *J. Am. Chem. Soc.*, 126, 34, pp. 10757-10762

Kim, S. M.; Pint, C. L.; Amama, P. B.; Hauge, R. H.; Maruyama, B. & Stach, E. A. (2010). Catalyst and catalyst support morphology evolution in single-walled carbon nanotube supergrowth: Growth deceleration and termination. *J. Mater. Res.*, 25, 10, pp. 1875-1885

Kreupl, F.; Graham, A. P.; Duesberg, G. S.; Steinhogl, W.; Liebau, M.; Unger, E. & Honlein, W. (2002). Carbon nanotubes in interconnect applications. *Microelectron. Eng.*, 64, 1-4, pp. 399-408

Lan, C.; Amama, P. B.; Fisher, T. S. & Reifenberger, R. G. (2007). Correlating electrical resistance to growth conditions for multiwalled carbon nanotubes. *Appl. Phys. Lett.*, 91, 9, pp. 093105-093107

Li, Y.; Mann, D.; Rolandi, M.; Kim, W.; Ural, A.; Hung, S.; Javey, A.; Cao, J.; Wang, D.; Yenilmez, E.; Wang, Q.; Gibbons, J. F.; Nishi, Y. & Dai, H. (2004). Preferential Growth of Semiconducting Single-Walled Carbon Nanotubes by a Plasma Enhanced CVD Method. *Nano Lett.*, 4, 2, pp. 317-321

Maruyama, S.; Einarsson, E.; Murakami, Y. & Edamura, T. (2005). Growth process of vertically aligned single-walled carbon nanotubes. *Chem. Phys. Lett.*, 403, 4-6, pp. 320-323

Maschmann, M. R.; Amama, P. B. & Fisher, T. S. (2005). Effect of DC Bias on Microwave Plasma Enhanced Chemical Vapor Deposition Synthesis of Single-Walled Carbon Nanotubes. *ASME Conference Proceedings*, 0-7918-4223-1 Orlando, Florida, (November, 2005)

Maschmann, M. R.; Franklin, A. D.; Amama, P. B.; Zakharov, D. N.; Stach, E. A.; Sands, T. D. & Fisher, T. S. (2006a). Vertical single- and double-walled carbon nanotubes grown from modified porous anodic alumina templates. *Nanotechnology*, 17, 15, pp. 3925-3929

Maschmann, M. R.; Franklin, A. D.; Scott, A.; Janes, D. B.; Sands, T. D. & Fisher, T. S. (2006b). Lithography-Free in Situ Pd Contacts to Templated Single-Walled Carbon Nanotubes. *Nano Lett.*, 6, 12, pp. 2712-2717

Maschmann, M. R.; Amama, P. B.; Goyal, A.; Iqbal, Z.; Gat, R. & Fisher, T. S. (2006c). Parametric study of synthesis conditions in plasma-enhanced CVD of high-quality single-walled carbon nanotubes. *Carbon*, 44, 1, pp. 10-18

Maschmann, M. R.; Amama, P. B.; Goyal, A.; Iqbal, Z. & Fisher, T. S. (2006d). Freestanding vertically oriented single-walled carbon nanotubes synthesized using microwave plasma-enhanced CVD. *Carbon*, 44, 13, pp. 2758-2763

Merkulov, V. I.; Melechko, A. V.; Guillorn, M. A.; Lowndes, D. H. & Simpson, M. L. (2001). Alignment mechanism of carbon nanofibers produced by plasma-enhanced chemical-vapor deposition. *Appl. Phys. Lett.*, 79, 18, pp. 2970-2972

Meyyappan, M.; Delzeit, L.; Cassell, A. & Hash, D. (2003). Carbon nanotube growth by PECVD: a review. *Plasma Sources Sci. Technol.*, 12, 2, pp. 205-216

Murakami, Y.; Chiashi, S.; Miyauchi, Y.; Hu, M.; Ogura, M.; Okubo, T. & Maruyama, S. (2004). Growth of vertically aligned single-walled carbon nanotube films on quartz substrates and their optical anisotropy. *Chem. Phys. Lett.*, 385, 3-4, pp. 298-303

Peng, H. B.; Ristroph, T. G.; Schurmann, G. M.; King, G. M.; Yoon, J.; Narayanamurti, V. & Golovchenko, J. A. (2003). Patterned growth of single-walled carbon nanotube arrays from a vapor-deposited Fe catalyst. *Appl. Phys. Lett.*, 83, 20, pp. 4238-4240

Pimenta, M. A.; Marucci, A.; Empedocles, S. A.; Bawendi, M. G.; Hanlon, E. B.; Rao, A. M.; Eklund, P. C.; Smalley, R. E.; Dresselhaus, G. & Dresselhaus, M. S. (1998). Raman modes of metallic carbon nanotubes. *Phys. Rev. B*, 58, 24, pp. R16016

Rakov, E. G. (2000). Methods for preparation of carbon nanotubes. *Russ. Chem. Rev.*, 69, 1, pp. 35-52

Rao, A. M.; Richter, E.; Bandow, S.; Chase, B.; Eklund, P. C.; Williams, K. A.; Fang, S.; Subbaswamy, K. R.; Menon, M.; Thess, A.; Smalley, R. E.; Dresselhaus, G. & Dresselhaus, M. S. (1997). Diameter-Selective Raman Scattering from Vibrational Modes in Carbon Nanotubes. *Science*, 275, 5297, pp. 187-191

Ural, A.; Li, Y. & Dai, H. (2002). Electric-field-aligned growth of single-walled carbon nanotubes on surfaces. *Appl. Phys. Lett.*, 81, 18, pp. 3464-3466

Yamamoto, K.; Akita, S. & Nakayama, Y. (1998). Orientation and purification of carbon nanotubes using ac electrophoresis. *J. Phys. D: Appl. Phys.*, 31, 8, pp. L34

Yeh, C. M.; Chen, M. Y.; Syu, J. S.; Gan, J. Y. & Hwang, J. (2006). Effect of gravity on the growth of vertical single-walled carbon nanotubes in a chemical vapor deposition process. *Appl. Phys. Lett.*, 89, 3, pp. 033117-033119

Yeh, C. M.; Chen, M. Y.; Gan, J.-Y.; Hwang, J.; Lin, C. D.; Chao, T. Y. & Cheng, Y. T. (2007). Effects of time on the quality of vertically oriented single-walled carbon nanotubes by gravity-assisted chemical vapour deposition. *Nanotechnology*, 18, 14, pp. 145613

Yen, J. H.; Leu, I. C.; Lin, C. C. & Hon, M. H. (2005). Synthesis of well-aligned carbon nanotubes by inductively coupled plasma chemical vapor deposition. *Applied Appl. Phys. A: Mater. Sci. Process.*, 80, pp. 415-421

Yen, J. H.; Leu, I. C.; Lin, C. C. & Hon, M. H. (2005). Synthesis of well-aligned carbon nanotubes by inductively coupled plasma chemical vapor deposition. *Appl. Phys. A*, 80, pp. 415-421

Zhang, G.; Mann, D.; Zhang, L.; Javey, A.; Li, Y.; Yeilmez, E.; Wang, Q.; Mcvittie, J. P.; Nishi, Y.; Gibbons, J. & Dai, H. (2005). Ultra-high-yield growth of vertical single-walled carbon nanotubes: Hidden roles of hydrogen and oxygen. *Proc. Natl. Acad. Sci.*, 102, 45, pp. 16141-16145

Zhang, Y. G.; Chang, A. L.; Cao, J.; Wang, Q.; Kim, W.; Li, Y. M.; Morris, N.; Yenilmez, E.; Kong, J. & Dai, H. (2001). Electric-field-directed growth of aligned single-walled carbon nanotubes. *J. Appl. Phys. Lett.*, 79, 19, pp. 3155-3157

Zhong, G. F.; Iwasaki, T.; Honda, K.; Furukawa, Y.; Ohdomari, I. & Kawarada, H. (2005). Very High Yield Growth of Vertically Aligned Single-Walled Carbon Nanotubes by Point-Arc Microwave Plasma CVD. *Chem. Vap. Deposition*, 11, 3, pp. 127-130

Zhu, Z.; Jiang, H.; Susi, T.; Nasibulin, A. G. & Kauppinen, E. I. (2010). The Use of NH3 to Promote the Production of Large-Diameter Single-Walled Carbon Nanotubes with a Narrow (n,m) Distribution. *J. Am. Chem. Soc.*, 133, 5, pp. 1224-1227
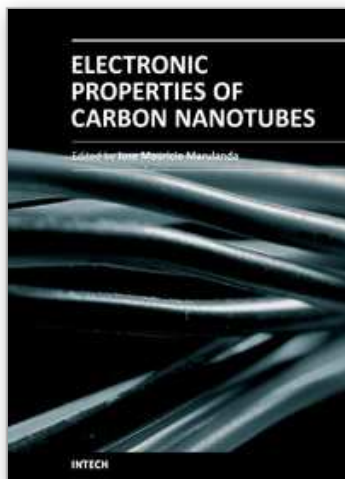
Electronic Properties of Carbon Nanotubes

Edited by Prof. Jose Mauricio Marulanda

Carbon nanotubes (CNTs), discovered in 1991, have been a subject of intensive research for a wide range of applications. These one-dimensional (1D) graphene sheets rolled into a tubular form have been the target of many researchers around the world. This book concentrates on the semiconductor physics of carbon nanotubes, it brings unique insight into the phenomena encountered in the electronic structure when operating with carbon nanotubes. This book also presents to reader useful information on the fabrication and applications of these outstanding materials. The main objective of this book is to give in-depth understanding of the physics and electronic structure of carbon nanotubes. Readers of this book should have a strong background on physical electronics and semiconductor device physics. This book first discusses fabrication techniques followed by an analysis on the physical properties of carbon nanotubes, including density of states and electronic structures. Ultimately, the book pursues a significant amount of work in the industry applications of carbon nanotubes.

How to reference

In order to correctly reference this scholarly work, feel free to copy and paste the following:

Matthew Maschmann, Timothy Fisher and Placidus Amama (2011). Enhanced Control of Single-Walled Carbon Nanotube Properties Using MPCVD with DC Electrical Bias, Electronic Properties of Carbon Nanotubes, Prof. Jose Mauricio Marulanda (Ed.), ISBN: 978-953-307-499-3, InTech, Available from: http://www.intechopen.com/books/electronic-properties-of-carbon-nanotubes/enhanced-control-of-single-walled-carbon-nanotube-properties-using-mpcvd-with-dc-electrical-bias

INTECH
open science | open minds